CHEMISTRY OF MATERIALS
Article

Chem. Mater. **2010,** *22,* 4505–4511 4505
DOI:10.1021/cm1013762

Enzyme-Cofactor-Assisted Photochemical Synthesis of Ag Nanostructures and Shape-Dependent Optical Sensing of Hg(II) Ions

Raj Kumar Bera, Ashok Kumar Das, and C. Retna Raj*

Department of Chemistry, Indian Institute of Technology, Kharagpur 721308, India

Received May 15, 2010. Revised Manuscript Received June 28, 2010

We describe a rapid green photochemical route for the synthesis of polyhedral Ag nanostructures, using the enzyme cofactor reduced nicotinamide adenine dinucleotide (NADH) and their analytical application in the optical sensing of environmentally hazardous Hg(II) ions at parts per billion (ppb) levels. Our synthetic methodology involves the reduction of Ag(I) ions by triplet-state NADH in aqueous solution. Quasi-spherical nanoparticles with an average size of 25 nm were obtained at the initial stage of the reaction. Light induces the transformation of quasi-spherical nanoparticles into a polyhedral nanostructure, with sizes ranging from 30 nm to 40 nm. The polyhedral nanostructures are highly stable for months in darkness and display two distinct surface plasmon bands, at 400 and 630 nm, corresponding to the quadrupole and dipole in-plane plasmon resonance, respectively. The polyhedral nanostructures are mainly composed of a (111) lattice plane with twinned boundaries. The thermodynamically favorable redox reaction of colloidal polyhedral Ag nanostructures with Hg(II) ions has been exploited for the optical sensing of Hg(II) in aqueous solution. The oxidative etching of polyhedral Ag nanostructures by Hg(II) ions strongly influences their optical characteristics: the deep green color of the colloidal Ag nanostructures changes to bright yellow. The surface plasmon band at the longer-wavelength side disappears in the presence of Hg(II) ions. The polyhedral Ag nanostructures transform to spherical nanoparticles because of oxidative etching. Sensing of Hg(II) ions at the ppb level has been achieved without any additional reagents. Our sensing method is very simple and highly selective; other common metal cations do not interfere with the measurement of Hg(II). The optical sensing capability of the Ag nanostructure is strongly dependent on their shape. The polyhedral Ag nanostructures have higher activity than the conventional spherical nanoparticles. Electrochemical studies supports the remarkable reactivity of polyhedral nanostructures toward Hg(II) ions. The polyhedral nanostructures are more susceptible to the oxidative etching reaction. The shape of the nanoparticle controls the oxidation potential of Ag nanostructures. The high reactivity of the polyhedral nanostructures is ascribed to the existence of defect sites.

Introduction

The synthesis of nanomaterials for various applications has received significant interest in the past two decades. The fascinating properties of these nanoscale materials originate from their quantum scale dimension and are exploited for applications in catalysis, biosensing, optoelectronics, etc.[1] The shape, size, and morphology of the nanomaterials have significant roles in controlling their properties. In principle, nanomaterials of desired properties can be synthesized by tuning their shape, size, and surface structure. The nanomaterials of different shapes and sizes have been synthesized using templates, structure-directing reagents, seeds, etc.[2] Traditional chemical methods involve the use of environmentally toxic or biologically hazardous reagents, solvents, etc. The aqueous citrate and borohydride reduction and two-phase Schiffrin synthetic routes are widely used to synthesize transition-metal nanoparticles.[3] The aqueous and nonaqueous methods involving structure-regulating reagents such as polymer, surfactants, nanoseeds, etc., and the polyol approach, are known to yield anisotropic metal nanostructures.[2,4] The increased emphasis on green

*Author to whom correspondence should be addressed. E-mail: crraj@chem.iitkgp.ernet.in.

(1) (a) Shipway, A. N.; Katz, E.; Willner, I. *ChemPhysChem*. **2000**, *1*, 18. (b) Wang, H.; Yang, R.; Yang, L.; Tan, W. *ACS Nano* **2009**, *3*, 2451. (c) Niemeyer, C. M. *Angew. Chem., Int. Ed.* **2001**, *40*, 4128. (d) Daniel, M. C.; Astruc, D. *Chem. Rev*. **2004**, *104*, 293. (e) Willner, I.; Baron, R.; Willner, B. *Adv. Mater*. **2006**, *18*, 1109.

(2) (a) Murphy, C. J.; Sau, T. K.; Gole, A. M.; Orendorff, C. J.; Gao, J.; Gou, L.; Hunyadi, S. E.; Li, T. *J. Phys. Chem. B* **2005**, *109*, 13857. (b) Pastoriza-Santos, I.; Liz-Marzan, L. M. *Adv. Funct. Mater*. **2009**, *19*, 679. (c) Xiao, Y.; Pavlov, V.; Levine, S.; Niazov, T.; Markovitch, G.; Willner, I. *Angew. Chem*. **2004**, *116*, 4619. (d) Lu, L.; Kobayashi, A.; Tawa, K.; Ozaki, Y. *Chem. Mater*. **2006**, *18*, 4894. (e) Skrablak, S. E.; Chen, J.; Sun, Y.; Lu, X.; Au, L.; Cobley, C. M.; Xia, Y. *Acc. Chem. Res*. **2008**, *41*, 1587. (f) Cushing, B. L.; Kolesnichenko, V. L.; O'Connor, C. *J. Chem. Rev*. **2004**, *104*, 3893. (g) Xue, C.; Mirkin, C. A. *Angew. Chem., Int. Ed*. **2007**, *46*, 2036. (h) Wiley, B. J.; Im, S. H.; Li, Z.-Y.; McLellan, J.; Siekkinen, A.; Xia, Y. *J. Phys. Chem. B*. **2006**, *110*, 15666.

(3) (a) Dong, X.; Ji, X.; Jing, J.; Li, M.; Li, J.; Yang, W. *J. Phys. Chem. C* **2010**, *114*, 2070. (b) Sun, Y.; Mayers, B.; Xia, Y. *Nano Lett*. **2003**, *3*, 675. (c) Jiang, X.; Zeng, Q.; Yu, A. *Langmuir* **2007**, *23*, 2218. (d) Zhang, S.; Leem, G.; Lee, T. R. *Langmuir* **2009**, *25*, 13855. (e) Reilly, S. M.; Krick, T.; Dass, A. *J. Phys. Chem. C* **2010**, *114*, 741. (f) Toikkanen, O.; Ruiz, V.; Ronnholm, G.; Kalkkinen, N.; Liljeroth, P.; Quinn, B. M. *J. Am. Chem. Soc*. **2008**, *130*, 11049.

(4) Wiley, B.; Herricks, T.; Sun, Y.; Xia, Y. *Nano Lett*. **2004**, *4*, 1733.

Published on Web 07/20/2010

chemistry demands an ecofriendly route for the synthesis of metal nanostructures. The photochemical approach offers a new route for the synthesis of metal nanostructures.[5−8] The photochemical route has several advantages over the other methods, such as high spatial resolution, in situ generation of reducing species, etc.[5−8] Scaiano's group extensively used the photochemical approach for the synthesis of metal nanoparticles.[6] Photochemically generated reactive intermediates effectively reduce metal ions and yield nanoparticles. Recently, they have elegantly demonstrated the morphology-controlled synthesis of Ag nanoparticles using light-emitting diodes (LEDs).[6e] Nishioka et al. synthesized Au nanorods via the photochemical reaction of ketones in an aqueous micellar solution.[7a] Balan et al. reported the in situ photochemical synthesis of Ag nanoparticles in a polymerizable acrylic formulation.[7b] Jradi et al. synthesized Ag nanowires via the photosensitized reduction of Ag(I) ions.[7c] The photochemical growth of water-soluble Au nanorods was recently achieved using Ag(I) and acetone.[7d] Mallick et al. reported the synthesis of Ag nanoparticles using the radical photochemically generated from methoxypolyethylene glycol.[8] The photoreduction of Ag(I) and the formation of Ag nanoparticles have been reported by several other groups.[9] The conventional photochemical methods for the synthesis of metal nanoparticles involves long-time ultraviolet (UV) irradiation and requires a polymer or surfactant to obtain stable nanoparticles. It is desirable to develop a rapid photochemical method involving a nontoxic solvent/stabilizer/sensitizer for the implementation of green synthetic strategy in the field of nanoscience.

Mercury is one of the heavy metals. It exists in three different forms: elemental mercury, methylmercury, and inorganic mercury.[10] Mercury is highly toxic and is a serious threat to the environment and human health. Hg(II), which is the stable form of mercury, has a high level of cellular toxicity and is carcinogenic.[11] Biomethylation of Hg(II) yields methylmercury and is accumulated in the body through the food chain, leading to several life-threatening diseases.[12] The high toxicity and associated health problems demand the detection of trace amounts of Hg(II) in drinking water, rivers, large water bodies, food, and soil. Spectral methods such as atomic absorption, fluorescence, and inductively coupled plasma spectrometric and voltammetric methods have been used for the detection of Hg(II).[13] The conventional methods require expensive equipment and special reagents. In recent years, the colorimetric methods based on the surface plasmon resonance of Au nanoparticles have been proven to be versatile for the detection of Hg(II).[14,15] The interaction of Hg(II) ions with DNA/oligonucletide functionalized Au/Ag nanoparticles has been extensively exploited for the sensing of Hg(II) by various groups.[15] Although these methods are highly sensitive and selective, suitable functionalization procedures must be followed without perturbing the optical characteristics of nanoparticles. Rapid, highly sensitive and selective inexpensive sensing methodology with simple protocol is desired for the on-site measurement of Hg(II)-contaminated samples.

Herein, for the first time, we describe (i) a new environmentally benign photochemical route for the synthesis of Ag nanostructures in an aqueous medium using the enzyme cofactor reduced nicotinamide adenine dinucleotide (NADH) and (ii) nanoparticle shape-dependent optical sensing of environmentally toxic Hg(II) ions at the parts per billion (ppb) level. Our synthetic method does not require any additional stabilizing agent; NADH functions both as a reducing and stabilizing agent. The

(5) (a) Jin, R. C.; Cao, Y. W.; Mirkin, C. A.; Kelly, K. L.; Schatz, G. C.; Zheng, J. G. *Science* **2001**, *294*, 1901. (b) An, J.; Tang, B.; Ning, X.; Zhou, J.; Xu, W.; Zhao, B.; Xu, W.; Corredor, C.; Lombardi, J. R. *J. Phys. Chem. C* **2007**, *111*, 18055. (c) Zhou, J.; An, J.; Tang, B.; Xu, S. P.; Cao, Y. X.; Zhao, B.; Xu, W. Q.; Chang, J. J.; Lomardi, J. R. *Langmuir* **2008**, *24*, 10407. (d) Miranda, O. R.; Ahmadi, T. S. *J. Phys. Chem. B* **2005**, *109*, 15724. (e) Quaresma, P.; Soares, L.; Contar, L.; Miranda, A.; Osorio, I.; Carvalho, P. A.; Franco, R.; Pereira, E. *Green Chem.* **2009**, *11*, 1889. (f) Jin, R.; Cao, Y. C.; Hao, E.; Métraux, G. S.; Schatz, G. C.; Mirkin, C. A. *Nature* **2003**, *425*, 487.

(6) (a) Marin, M. L.; McGilvray, K. L.; Scaiano, J. C. *J. Am. Chem. Soc.* **2008**, *130*, 16572. (b) Maretti, L.; Billon, P. S.; Liu, Y.; Scaiano, J. C. *J. Am. Chem. Soc.* **2009**, *131*, 13972. (c) Gonzalez, C. M.; Liu, Y.; Scaiano, J. C. *J. Phys. Chem. C* **2009**, *113*, 11861. (d) McGilvray, K. L.; Decan, M. R.; Wang, D.; Scaiano, J. C. *J. Am. Chem. Soc.* **2006**, *128*, 15980. (e) Stamplecoskie, K. G.; Scaiano, J. C. *J. Am. Chem. Soc.* **2010**, *132*, 1825. (f) Scaiano, J. C.; Aliaga, C.; Maguire, S.; Wang, D. *J. Phys. Chem. B* **2006**, *110*, 12856.

(7) (a) Nishioka, K.; Niidome, Y.; Yamada, S. *Langmuir* **2007**, *23*, 10353. (b) Balan, L.; Turck, C.; Soppera, O.; Vidal, L.; Lougnot, D. J. *Chem. Mater.* **2009**, *21*, 5711. (c) Jradi, S.; Balan, L.; Zeng, X. H.; Plain, J.; Lougnot, D. J.; Royer, P.; Bachelot, R.; Akil, S.; Soppera, O.; Vidal, L. *Nanotechnology* **2010**, *21*, 095605. (d) Placido, T.; Comparelli, R.; Giannici, F.; Cozzoli, P. D.; Capitani, G.; Striccolli, M.; Agostiano, A.; Currit, M. L. *Chem. Mater.* **2009**, *21*, 4192.

(8) Mallick, K.; Witcomb, M. J.; Scurrell, M. S. *J. Mater. Sci.* **2004**, *39*, 4459.

(9) (a) Veletanlic, E.; Goh, M. C. *J. Phys. Chem. C* **2009**, *113*, 18020. (b) Cui, X.; Li, C. M.; Bao, H.; Zheng, X.; Zang, J.; Ooi, C. P.; Guo, J. *J. Phys. Chem. C* **2008**, *112*, 10730. (c) Zhao, Y.; Qi, W.; Li, W.; Wu, L. *Langmuir* **2010**, *26*, 4437. (d) Lee, S. J.; Piorek, B. D.; Meinhart, C. D.; Moskovits, M. *Nano Lett.* **2010**, *10*, 1329. (e) Liu, Y.; He, L.; Xu, C.; Han, M. *Chem. Commun.* **2009**, 6566. (f) Maillard, M.; Huang, P.; Brus, L. *Nano Lett.* **2003**, *3*, 1611.

(10) Hylander, L. D.; Goodsite, M. E. *Sci. Total Environ.* **2006**, *368*, 352.

(11) (a) World Health Organization. *Environmental Health Criteria 118: Inorganic Mercury*; World Health Organization: Geneva, Switzerland, 1991. (b) McKeown-Eyssen, G. E.; Ruedy, J.; Neims, A. *Am. J. Epidemol.* **1983**, *118*, 470.

(12) Wojcik, D. P.; Godfrey, M. E.; Christie, D.; Haley, B. E. *Neuroendocrinol. Lett.* **2006**, *27*, 415.

(13) (a) Salaun, P.; van den Berg, C. M. G. *Anal. Chem.* **2006**, *78*, 5052. (b) Nolan, E. M.; Lippard, S. J. *J. Am. Chem. Soc.* **2003**, *125*, 14270. (c) Powell, M. J.; Quan, E. S. K.; Boomer, D. W.; Wiederin, D. R. *Anal. Chem.* **1992**, *64*, 2253. (d) Wang, Z.; Lee, J. H.; Lu, Y. *Chem. Commun.* **2008**, 6005. (e) Ono, A.; Togashi, H. *Angew. Chem., Int. Ed.* **2004**, *43*, 4300. (f) Liu, J. W.; Lu, Y. *Angew. Chem., Int. Ed.* **2007**, *46*, 7587. (g) Chiang, C.-K.; Huang, C.-C.; Liu, C.-W.; Chang, H.-T. *Anal. Chem.* **2008**, *80*, 3716. (h) Fan, Y.; Liu, Z.; Wang, L.; Zhan, J. *Nanoscale Res. Lett.* **2009**, *4*, 1230.

(14) (a) Darbha, G. K.; Singh, A. K.; Rai, U. S.; Yu, E.; Yu, H. T.; Ray, P. C. *J. Am. Chem. Soc.* **2008**, *130*, 8038. (b) Rex, M.; Hernandez, F. E.; Campiglia, A. D. *Anal. Chem.* **2006**, *78*, 445.

(15) (a) Lee, J. S.; Han, M. S.; Mirkin, C. A. *Angew. Chem., Int. Ed.* **2007**, *46*, 4093. (b) Liu, C. W.; Hsieh, Y. T.; Huang, C. C.; Lin, Z. H.; Chang, H. T. *Chem. Commun.* **2008**, 2242. (c) Xue, X.; Wang, F.; Liu, X. *J. Am. Chem. Soc.* **2008**, *130*, 3244. (d) Li, D.; Wieckowska, A.; Willner, I. *Angew. Chem., Int. Ed.* **2008**, *47*, 3927. (e) Lee, J. S.; Mirkin, C. A. *Anal. Chem.* **2008**, *80*, 6805. (f) Ye, B. C.; Yin, B. C. *Angew. Chem., Int. Ed.* **2008**, *47*, 8386. (g) He, S.; Li, D.; Zhu, C.; Song, S.; Wang, L.; Long, Y.; Fan, C. *Chem. Commun.* **2008**, 4885.

photoexcited NADH in its triplet state efficiently reduces Ag(I) ions and produces nanoscale Ag particles. The sensing method described herein stems from the thermodynamically favorable redox reaction between Ag nanoparticles and Hg(II) ions. This method is highly selective, very sensitive, and requires no additional reagents.

Materials and Methods

Materials. $AgNO_3$, $Hg(NO_3)_2$, and NADH were purchased from Sigma−Aldrich. All other chemicals used in this investigation were analytical grade and used without further purification. All the solutions were prepared with purified water (Milli-Q system, Millipore, Bedford, MA).

Instrumentation. Electronic absorption spectra were recorded with a Cary Model 5000 UV−visible-NIR spectrophotometer. Transmission electron microscopy (TEM) images were acquired using JEOL Model JEM-2010 microscopes with an operating voltage of 200 kV. For compositional analysis, energy-dispersive X-ray spectroscopy (EDX) measurements were performed. XRD patterns of the samples were collected using Panalytical X'pert PRO XRD unit with nickel-filtered Cu Kα radiation (λ = 1.54 Å). Electrochemical experiments were performed with a Model CHI643B electrochemical analyzer (CHI). A two-compartment, three-electrode electrochemical cell with a glassy carbon (GC) working electrode, a Ag/AgCl (3 M NaCl) reference electrode, and Pt wire auxiliary electrodes were used in the electrochemical studies. All the potentials are referenced against NHE, unless mentioned otherwise.

Synthesis of Ag Nanostructures. In a typical synthesis, 150 μL of $AgNO_3$ (20 mM) was mixed with 1.2 mL of NADH (5 mM) and 1.65 mL of Millipore purified water. The reaction mixture was then irradiated using a 150-W sun lamp with a spectral output of >350 nm. The glass vial was kept at a distance of 10 cm from the light source, to avoid heating the solution. A series of color changes was noticed during the course of the reaction. The colorless reaction mixture turns yellow within 5 min, and it turns orange within 10 min; the color changes to deep red after 20 min and bluish green after 25 min, and, finally, the bluish green changes to deep green after 30 min. The deep-green-colored nanoparticles obtained at the end of the reaction was stored in darkness and was stable for months. The citrate-stabilized spherical Ag nanoparticles were synthesized according to the literature procedure with little modification.[5b] Briefly, 60 μL of aqueous $NaBH_4$ solution (21 mM) was added dropwise to an aqueous mixture of sodium citrate (0.5 mM) and $AgNO_3$ (0.3 mM) under vigorous stirring. The bright yellow Ag nanoparticle obtained was stored at room temperature.

Optical Sensing of Hg(II). Sensing of the Hg(II) ions was performed in aqueous solution. Because the absorbance of the as-synthesized Ag nanoparticle is significantly high, it was quantitatively diluted (4 times) with Millipore purified water before using in the sensing experiments. Typically, an aqueous solution of Hg(II) (5 μL of 0.03 mM) was gradually added to the diluted colloidal Ag nanoparticle (3 mL) sample and the spectrum was recorded after 2 min.

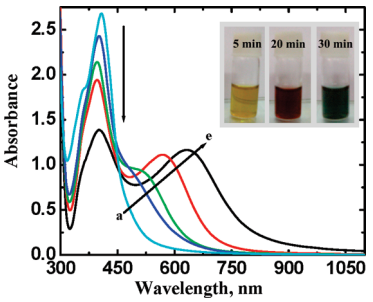

Figure 1. Time-dependent spectral profile obtained during the photochemical synthesis of Ag nanostructures ([$AgNO_3$], 1 mM; [NADH], 2 mM). Time: (a) 5, (b) 10, (c) 15, (d) 20, and (e) 30 min. The spectra were recorded after diluting the original colloidal sample four times. Inset shows photographs of the nanoparticles obtained after 5, 20, and 30 min of irradiation.

Electrochemical Measurements. The GC electrodes were repeatedly polished with an alumina slurry and washed extensively with water in a sonicator bath. The as-synthesized colloidal Ag nanoparticles (20 μL) were dropcast onto the cleaned GC electrode, dried at room temperature for 30 min, and then subjected to electrochemical experiments. An aqueous solution of H_2SO_4 (0.5 M) was used as the electrolyte solution, and the electrochemical experiment was performed under an argon atmosphere. All the experiments were repeated at least three times, and similar results were obtained.

Results and Discussion

The synthesis of anisotropic Ag nanostructures involves the reduction of Ag^+ by photoexcited NADH in its triplet state. The progress of the reaction was monitored by spectral and electron microscopic measurements. A series of color changes was observed during the growth of the Ag nanostructures (Figure 1). First, the colorless reaction mixture became bright yellow within 5 min of the start of the reaction. The yellow color changed to orange (after 10 min) and then to red (after 20 min). The red color turned bluish-green within 25 min, and finally a deep green color was developed at the end of the reaction (30 min). The absorption spectra, obtained at different irradiation times, are shown in Figure 1. One main absorption band (at ~407 nm) and a small shoulder band at a shorter wavelength (~360 nm) were observed in the initial stage (5 min) of the reaction (see Figure 1). A significant decrease in the absorbance of the band at 407 nm and the birth of an additional shoulder band at ~500 nm were noticed as the irradiation time increased. The absorbance of the newborn shoulder-like band increased with time, and the band position shifted further to a longer-wavelength region. This band stabilized at 630 nm after 30 min of irradiation. No further change in the spectral profile was noticed after 30 min of the reaction. The spectrum obtained after the completion of the reaction exhibits two bands, at 400 and 630 nm, corresponding to the quadrupole and dipole in-plane plasmon resonance, respectively.[5a,b] Mie's theory predicts that

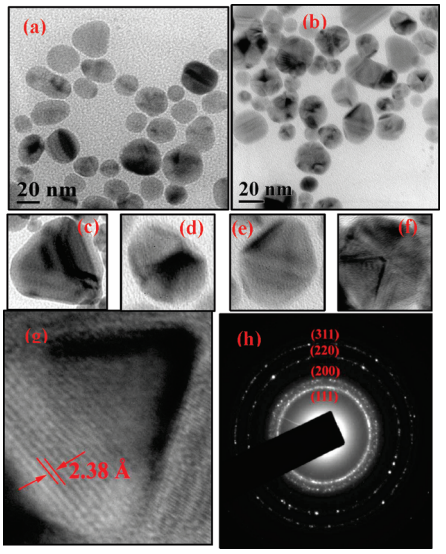

Figure 2. TEM images of the Ag nanostructure obtained (a) 5 and (b) 30 min after the start of the reaction. Selected polyhedral Ag nanostructures are shown in panels (c), (d), (e), and (f). The HRTEM and SAED pattern are respectively shown in panels (g) and (h).

the spherical nanoparticle would display a single plasmon band, whereas the anisotropic nanostructures can exhibit more than one band, depending on their shape.[16] The spectral profile shown in Figure 1 indicates that the nanoparticles are anisotropic in nature. The red-shift in the newborn band with irradiation time may be ascribed to the formation of nanostructures with sharp corners or edges.[2h] The growth of newborn band at the expense of the band at 407 nm suggests the transformation of the nanoparticles produced at the initial stage of the reaction. The irradiation of the sample in the absence of NADH does not show any of these spectral features, indicating the involvement of NADH in the reduction of Ag(I).

Figure 2 shows TEM images of Ag nanostructures obtained at different stages of the reaction. The shape of the nanostructures strongly depends on the irradiation time. The sample irradiated for 5 min shows quasispherical and ellipsoidal Ag nanostructures, with an average size of 25 nm. On the other hand, the sample irradiated for 30 min has polyhedral-shaped nanoparticles with sizes ranging from 30 nm to 40 nm. The nanoparticles are polydispersed and do not have uniform shape. It is likely that the spherical and ellipsoidal nanoparticles formed at the initial stages of the reaction transform to nanoparticles of other shapes with time. The close examination of the TEM image reveals that the nanoparticles have tetrahedral, pyramidal, octahedral, and penta-twinned decahedral shapes (see Figures 2c−f). The HRTEM image of the nanostructures (Figure 2g) shows the fringe spacing of 2.38 Å, corresponding to the interplanar spacing between (111) planes. The selected-area electron diffraction (SAED) pattern was indexed to the (111), (200), (220), and (311) planes of a face-centered cubic (FCC) lattice. The XRD pattern recorded for the nanoparticles further confirms the existence of such planes (see Figure 1S in the Supporting Information). The spectral profile and TEM images obtained at different time intervals indicate that light plays two important roles: (i) it triggers the reaction of NADH with Ag(I) ions to form Ag(0) and (ii) it induces the transformation of quasi-spherical nanoparticles to polyhedral nanostructures. The nanoparticles with favorable polyhedral geometry are believed to evolve from the quasi-spherical nanoparticles that are formed at the initial stage of the reaction. The plasmon excitation is known to induce a structural transition on the nanoscale particles.[5f,6f,17,18] The excitation wavelength can strongly influence the size and morphology of Ag nanoparticles.[6f,18] However, these methodologies require long irradiation time (7−70 h) for the transformation of spherical nanoparticles.[5a,5b,5f,18] For instance, Jin et al. observed the plasmon-induced transformation of Ag nanospheres to nanoprisms after 50−70 h of irradiation.[2g,5f] Interestingly, in our case, the transformation of the spherical/ellipsoidal nanoparticles to polyhedral structures is very fast (30 min), suggesting that NADH also plays a role in the shape evolution. The stabilizing effect of NADH favors the evolution of polyhedral nanostructures.

Scheme 1. Proposed Scheme Illustrating the Photochemical Reduction of Ag(I) and the Growth of Polyhedral Ag Nanostructures

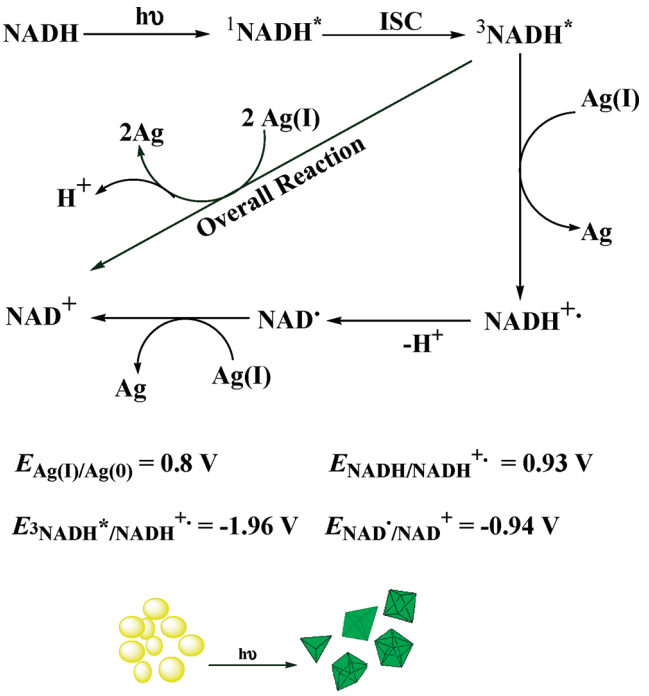

The reduction of Ag(I) by NADH does not proceed in darkness, and the reaction is very slow in room light, indicating that light controls the reduction of Ag(I) and the growth of nanoparticles. The reduction of Ag(I) is believed to occur according to the reaction mechanism proposed in Scheme 1. The NADH in the ground state is not capable of reducing Ag(I), because the redox potential

(16) Mie, G. *Ann. Phys.* **1908**, *25*, 377.
(17) Yacaman, M. J.; Ascencio, J. A.; Liu, H. B.; Gardea-Torresdey, J. *J. Vac. Sci. Technol. B* **2001**, *19*, 1091.
(18) Zheng, X.; Zhao, X.; Guo, D.; Tang, B.; Xu, S.; Zhao, B.; Xu, W. *Langmuir* **2009**, *25*, 3802.

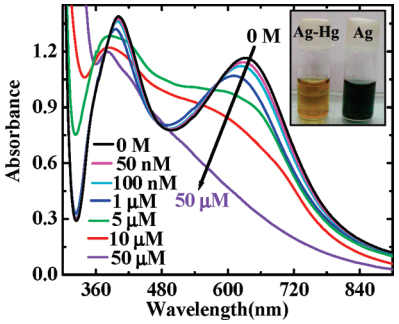

Figure 3. Optical spectra of polyhedral Ag nanostructures obtained at different concentrations of Hg(II) ions. Inset shows a photograph of colloidal Ag nanoparticles in the absence and presence of Hg(II) (50 μM).

of the NADH/NADH$^{+\bullet}$ couple (0.93 V)[19] is higher than that of the Ag(I)/Ag(0) couple (0.8 V). The absorption spectrum of NADH shows a strong band in the UVA region (340 nm) (see Figure 2S in the Supporting Information). The irradiation of NADH with a sun lamp would generate ^{1}NADH*, which is known to easily undergo intersystem crossing (ISC) to yield ^{3}NADH*.[20] The redox potential of ^{3}NADH* is reported to be -1.96 V,[20] which is significantly lower than the reduction potential of the Ag(I)/Ag(0) couple and, hence, the reduction of Ag(I) by ^{3}NADH* is a favorable process. The one-electron transfer reaction between Ag(I) and ^{3}NADH* generates Ag(0) and the cation radical NADH$^{+\bullet}$. The latter species can easily undergo deprotonation and yield the radical NAD$^\bullet$,[19b] which reacts with another Ag(I) ion to produce Ag(0) and NAD$^+$. The redox potential of the NAD$^\bullet$/NAD$^+$ couple (-0.94 V)[19a] favors the electron transfer reaction between NAD$^\bullet$ and Ag(I). The formation of NAD$^+$ was confirmed by spectral measurement; the supernatant of the colloidal nanoparticles shows a characteristic spectral signature for NAD$^+$ (see Figure 2S in the Supporting Information). The photochemically generated Ag(0) nucleate to yield quasi-spherical Ag nanoparticles at the initial stage. Continuous irradiation of the sample induces the transformation of the quasi-spherical morphology to a polyhedral-shaped nanoparticle.

Optical Sensing of Hg(II). The optical sensing of Hg(II) was achieved by taking advantage of the redox reaction between Hg(II) ions and Ag(0). Hg(II) ions are thermodynamically capable of oxidizing metallic Ag, because the redox potential of the Hg(II)/Hg couple (0.85 V) is higher than that of the Ag(I)/Ag couple (0.8 V). The Hg(II) ions can favorably interact with the Ag nanoparticles.[21] The oxidation of Ag nanoparticles by Hg(II) ions would strongly influence its optical characteristics, and the change in the surface plasmon band can be used to quantify the concentration of Hg(II). Figure 3 is the optical spectra obtained for the polyhedral Ag nanoparticles in the presence of various concentrations of Hg(II) ions. The longer-wavelength band is highly sensitive toward

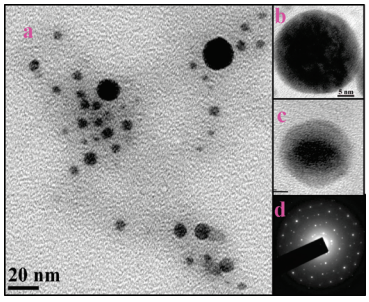

Figure 4. (a) TEM image of the Ag nanoparticles obtained after the addition of Hg(II) ions (50 μM). The selected HRTEM images (panels (b) and (c)) and SAED pattern (panel (d)) obtained for the Ag nanoparticles after their exposure to Hg(II) (samples collected after Hg(II) sensing) are shown in the insets.

Hg(II) ions. A gradual decrease in the absorbance and a significant blue shift in the band position were noticed when the concentration of Hg(II) ions was increased. A small decrease in the absorbance and a slight blue shift in the transverse band were also noticed in the presence of Hg(II). At high concentrations of Hg(II), the longer-wavelength band completely vanished and only one band (at ~380 nm) was observed. The deep green color of the colloidal Ag nanostructure turned bright yellow, which is characteristic of spherical Ag nanoparticles upon the addition of Hg(II) ions. The decrease in the absorbance or shift in the position of the longer-wavelength band is a direct measure of the concentration of Hg(II) ions. The lowest concentration of Hg(II) quantified was 9 ppb (50 nM). The remarkable blue shift in the longer-wavelength band and its disappearance at high concentrations of Hg(II) can be ascribed to a significant change in the morphology of the particles. The disappearance of the longer-wavelength band upon the addition of Hg(II) points out the transformation of polyhedral nanoparticle to nanoparticles of other shapes and morphology by the partial oxidation of the nanoparticles. The TEM image (Figure 4) obtained for the Ag nanoparticles exposed to Hg(II) ions confirms (i) the transformation of twinned polyhedral nanoparticles into spherical and quasi-spherical nanoparticles, (ii) oxidative etching or dissolution of the Ag nanostructures, and (iii) a significant decrease in the initial size of the nanostructures. The redox reaction between Ag nanostructures and Hg(II) ions transform the polyhedral shape to nanoparticles of spherical or quasi-spherical shape by oxidative etching. The distribution of nanoparticles size and shape before and after their exposure to Hg(II) was obtained from the TEM measurements. These nanoparticles have sizes ranging from 5 nm to 20 nm. The majority of the nanoparticles have sizes of < 10 nm (see Figure 3S in the Supporting Information). Almost all the nanoparticles have the spherical/ellipsoidal shape. The SAED measurement shows a spotty pattern, indicating that the nanoparticles are single crystalline (see Figure 4). The XRD profile and energy-dispersive spectral pattern show the signatures for Ag and Hg (see Figures 4S and 5S, respectively, in the Supporting Information). In the XRD profile, the intensity of the Ag(111) plane significantly decreased with

(19) (a) Zhu, X.-Q.; Yang, Y.; Zhang, M.; Cheng, J.-P. *J. Am. Chem. Soc.* **2003**, *125*, 15298. (b) Carlson, B. W.; Miller, L. L.; Neta, P.; Grodkowski, J. *J. Am. Chem. Soc.* **1984**, *106*, 7233.
(20) Tanaka, M.; Ohkubo, K.; Fukuzumi, S. *J. Phys. Chem. A* **2006**, *110*, 11214.
(21) Henglein, A.; Brancewicz, C. *Chem. Mater.* **1997**, *9*, 2164.

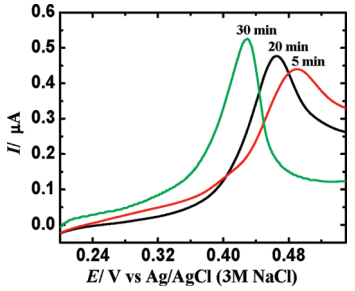

Figure 5. Linear sweep voltammograms for the oxidation of Ag nanostructures obtained at different reaction times. Supporting electrolyte: 0.1 M H_2SO_4. Scan rate = 100 mV/s.

respect to the original XRD pattern of the polyhedral Ag nanoparticles. The Ag(I) ions produced by the partial oxidation of the Ag nanoparticle by Hg(II) was tested by adding Cl^- ions to the nanoparticle supernatant. The formation of AgCl was noticed, confirming the presence of Ag(I) ions. Two probable reactions of Hg(0) formed by the redox reaction can be considered: (i) surface coating of polyhedral nanostructures with zerovalent Hg and (ii) formation of amalgam between the Hg and Ag nanoparticles. The coexistence of both of these processes cannot be ruled out. Because Hg is slightly more electropositive than Ag, it can favorably interact with Ag.[21] Katsikas et al. and Moris et al.[22] reported that the adsorption of Hg onto Ag nanoparticles causes a blue shift in the surface plasmon band of the nanoparticles. The HRTEM image obtained for the Ag nanostructures after its exposure to Hg(II) suggests the adsorption of Hg on the surface of Ag nanoparticles (Figure 4).

Shape-Dependent Optical Sensing. The optical response of the colloidal Ag nanoparticles relative to Hg(II) strongly depends on the shape of the nanoparticle. The polyhedral Ag nanostructures are highly sensitive to trace amounts of Hg(II) ions. However, the quasi-spherical nanoparticles obtained after 5 min of irradiation do not show any observable changes relative to Hg(II) in the low concentration range (0−5 μM) (see Figure 6S in the Supporting Information). Moreover, the conventional citrate-stabilized spherical Ag nanoparticle also does not respond to Hg(II) in the low concentration range (see Figure 7S in the Supporting Information). A change in the absorbance of these spherical nanoparticles was noticed only at high concentrations of Hg(II) (> 5 μM). The polyhedral nanoparticles obtained at longer irradiation times (20−30 min) only show significant changes in the spectral profile, even in the presence of trace amounts of Hg(II), demonstrating that the shape of the Ag nanostructure has great control over the redox reaction and polyhedral Ag has high activity. The high activity of polyhedral nanostructures toward Hg(II) originates from the large number of defect sites. The nanoparticles with twinned morphology have relatively

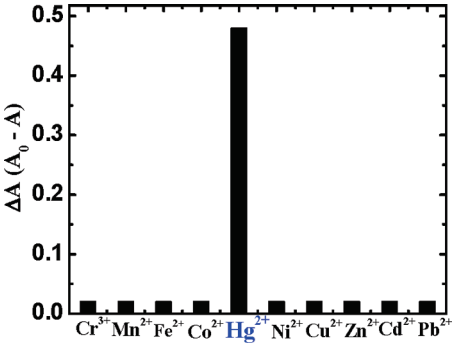

Figure 6. Plot illustrating the selectivity of the optical sensing method toward Hg(II). Change in the absorbance is plotted against the metal cations.

higher activity for oxidative etching, because of the presence of inherent defects.[2h,4,23] The defects provide high-energy sites and strongly favor the oxidative dissolution of the twinned nanostructures.[4] The redox reaction preferentially occurs at the edges and corners of the polyhedral nanostructures, because of the high surface energy at the edges and corners. Consequently, the polyhedral shape of the nanoparticles changes to quasi-spherical. The spherical or quasi-spherical Ag nanoparticles are less reactive, with respect to the polyhedral nanostructures, presumably because of the absence or presence of fewer defect sites.

Electrochemical experiments have been performed to confirm the high-reactivity polyhedral Ag nanostructures. Figure 5 shows the linear sweep voltammograms of Ag nanostructures obtained at three different irradiation times (5, 20, and 30 min). The voltammetric peaks shown here corresponds to the one-electron oxidation of Ag to Ag(I). As can be readily seen, the oxidation potential strongly depends on the shape of the nanoparticle. The oxidation of the polyhedral Ag nanostructure occurs at a much-less-positive potential than that of the quasi-spherical nanostructures. The shape-dependent electrochemical behavior of Au nanostructures was demonstrated recently by Ming et al.[24] The oxidation potential of tetrahexahedral Au nanoparticles is less than that of the elongated Au nanostructure.[24] It is well-known that the atoms at the step edges with low coordination are significantly more active than those of the conventional nanoparticles.[24,25] Our electrochemical measurements show that the anodic peak potential (E_p) for the oxidation of the polyhedral Ag nanostructure is significantly less positive (~60 mV) than that of the quasi-spherical/ellipsoidal nanostructures, implying that the oxidation of polyhedral Ag nanostructures is more favorable than the spherical nanostructures. In such a situation, the reduction of Hg(II) ions is highly favorable by the polyhedral Ag nanostructure.

The optical sensing of Hg(II) using a polyhedral Ag nanostructure is highly selective. The selectivity of the assay was evaluated using the spectra of other metal

(22) (a) Katsikas, L.; Gutierrez, M.; Henglein, A. *J. Phys. Chem.* **1996**, *100*, 11203. (b) Morris, T.; Copeland, H.; McLinden, E.; Wilson, S.; Szuewski, G. *Langmuir* **2002**, *18*, 7261.
(23) An, J.; Tang, B.; Zheng, X.; Zhou, J.; Dong, F.; Xu, S.; Wang, Y.; Zhao, B.; Xu, W. *J. Phys. Chem. C* **2008**, *112*, 15176.
(24) Ming, T.; Feng, W.; Tang, Q.; Wang, F.; Sun, L.; Wang, J.; Yan, C. *J. Am. Chem. Soc.* **2009**, *131*, 16350.
(25) Cortie, M. B.; van der Lingen, E. *Mater. Forum* **2002**, *26*, 1.

cations, such as Cr^{3+}, Mn^{2+}, Fe^{2+}, Co^{2+}, Ni^{2+}, Cu^{2+}, Zn^{2+}, Cd^{2+}, and Pb^{2+}. No characteristic change in the spectral profile was obtained in the presence of these metal ions (see Figure 6), confirming the remarkable selectivity of the sensing method. Unlike Hg(II), these metal cations are not thermodynamically capable of oxidizing Ag nanostructures. Because the redox potentials of these cations are lower than that of the Ag(I)/Ag(0) couple, the oxidative etching reaction cannot be expected.

Conclusion

In conclusion, we have demonstrated a novel, ecofriendly photochemical route for the synthesis of a polyhedral Ag nanostructure using an enzyme cofactor and the optical sensing of environmentally hazardous Hg(II) ions. Our synthetic methodology does not require seeds, surfactant, or stabilizer. The photoexcited enzyme cofactor nicotinamide adenine dinucleotide (NADH), in its triplet excited state, assists in the reduction of Ag(I) ions and light induces the transformation of quasi-spherical nanoparticles formed at the initial stage of the reaction to a polyhedral shape. The photoexcited NADH, in its triplet state, can be used as an effective reducing agent for the rapid synthesis of anisotropic Ag nanoparticles. The nanoparticle is stable for months in darkness. This photochemical route is rapid, and anisotropic Ag nanostructures can be obtained within 30 min. The potential application of the Ag nanostructures in the optical sensing of Hg(II) is demonstrated. The optical sensing is based on the redox reaction between polyhedral Ag nanostructures and Hg(II) ions, and it is strongly dependent on the shape of the Ag nanostructure. This optical method is highly sensitive, and other metal cations do not interfere with the measurement. The surface structure and shape controls the redox reaction. The shape-dependent redox property of the nanostructures can be exploited for various catalytic applications. The polyhedral Ag nanostructure functions as an excellent optical probe in the sensing of Hg(II) ions.

Acknowledgment. This work was financially supported by Department of Science and Technology and Indian Institute of Technology. R.K.B. is a recipient of a UGC Fellowship. We thank Professor Rajakumar Ananthakrishnan (Department of Chemistry, IIT Kharagpur), for providing us the sunlamp facility, and Professor Chacko Jacob (Material Science Centre, IIT Kharagpur), for fruitful discussions on TEM analysis.

Supporting Information Available: XRD profile obtained for the polyhedral Ag nanoparticles before and exposure to Hg(II); absorption spectra for NADH, NAD^+, the supernatant, the addition of Hg(II) after 5 min of irradiation, and the citrate-stabilized spherical nanoparticle; EDX pattern of Ag nanoparticles after the addition of Hg(II); and a plot illustrating the particle size/shape distribution before and after exposure of the Ag nanoparticles to Hg(II). (PDF) This information is available free of charge via the Internet at http://pubs.acs.org/.